Journal of Applied Chemistry JAC http://chemistry.journals.semnan.ac.ir

Synthesis, crystal structure and Hirshfeld surface analysis of new phosphoric triamide [2-F-$C_6H_4C(O)NH]P(O)[NHCH(CH_3)_2]_2$

Atekeh Tarahhomi[a,*], Arnold L. Rheingold[b], James A. Golen[b]
[a]*Department of Chemistry, Semnan University, Semnan 35351-19111, Iran*
[b]*Department of Chemistry, University of California, San Diego, 9500 Gilman Drive, La Jolla, CA 92093, USA*

Article history:
Received: 21/Nov/2016
Received in revised form: 3/Feb/2017
Accepted: 11/ Feb /2017

Abstract

In present work, new phosphoric triamide *N*-(2-fluorobenzoyl)-*N′*,*N*"-diisopropylphosphoric triamide, [2-F-$C_6H_4C(O)NH]P(O)[NHCH(CH_3)_2]_2$, was synthesized and characterized by X-ray crystallography analysis. The asymmetric unit consists of two independent molecules P1 and P2 which aggregate through N_{CP}—H···O═C and $(N—H)_2$···O═P hydrogen bonds, forming two independent chains parallel to the *a* axis and giving $R_2^2(10)/R_2^1(6)$ loops. For further investigation on intermolecular interactions in the studied compound, 3D Hirshfeld surfaces (HSs) mapped with d_{norm} and corresponding 2D fingerprint plots (FPs) were employed for two molecules P1 and P2. Hirshfeld surface analysis shows that the H···H (62.3% of total Hirshfeld surface area for molecule P1 and 62.8% for P2), H···O/O···H (13.1% for P1 and 12.8 % for P2), H···C/C···H (12.4% for P1 and 12.7 % for P2) and H···F/F···H (8.2% for P1 and 7.8 % for P2) contacts are the dominant intermolecular interactions in the crystal structure.

Keywords: Phosphoric triamide, X-ray crystallography analysis, N—H···O Hydrogen bond, 3D Hirshfeld surface, 2D fingerprint plot.

1. Introduction

Phosphoric triamides with the basic part $P(O)[N]_3$ are an important family of phosphoramide compounds because of their applications in biochemistry [1], anticancer prodrugs [2] and their use as *O*-donor ligands [3,4]. Accordingly, nowadays the research on the preparation of phosphoric triamides with different amido fragments becomes a matter of great interest [5–7].

As study on the intermolecular interactions in the crystal structures is one of the favorite topics for the researchers, Hirshfeld surface analysis can be a good graphical tool for studying such interactions providing quantitative and visual information [8,9]. In the case of phosphoric triamides, Hirshfeld surface analysis has been used to study intermolecular interactions in a few crystal structures [6]. Whereas, such analysis by the graphical representations based on Hirshfeld surfaces

*. **Corresponding Author:** *E-mail address: tarahhomi.at@semnan.ac.ir; Tel.: +(98)2331533199*

and corresponding fingerprint plots comprehensively recognize the intermolecular interactions involved in crystal packing.

In the previous works, we have been reported the synthesis and crystal structures of the phosphoric triamides [2-F-$C_6H_4C(O)NH]P(O)[X]_2$ (X = $NHC_6H_4(4\text{-}CH_3)$ [10], $N(C_2H_5)_2$ [11], $N(CH_3)C_6H_{11}$ [12]). In this paper, we present the crystal structure of the new phosphoric triamide [2-F-$C_6H_4C(O)NH]P(O)[NHCH(CH_3)_2]_2$. The structural features and hydrogen bond pattern are studied. Moreover, the 3D Hirshfeld surfaces (HSs) and 2D fingerprint plots (FPs), using the program *Crystal Explorer* 3.1 [13], are investigated in order to visualize and study intermolecular interactions in the molecular crystal. The results of this study reveal the characteristic close intermolecular contacts H···H, H···O/O···H, H···C/C···H and H···F/F···H in the crystal structure.

2. Experimental procedure

2.1. Materials and Methods

All chemicals were of analytical grade, obtained from commercial sources and used without further purification. X-ray data for structure were collected on a Bruker *SMART* CCD [14] system with Cu *K*α rotating anode. Data were corrected for absorption with *SADABS* [15,16]. Structure refinement was carried out with *SHELXL-97* [17]. Structure was solved by direct methods with *SHELXS-97* and all non-H atoms were refined anisotropically by Fourier full-matrix least-squares on F^2.

Carbon atoms C9, C10, C25, C27 and C28 of isopropyl group were disordered over two positions with 50.1 and 49.9% occupancy while carbon C12 exhibited 73.5 and 26.5% occupancy. Fluorine atoms (F1, F1A and F2, F2A) were disorder over two positions and refined with occupancy set at 87.0 and 13.0% and the corresponding overlapping hydrogen atoms (H1A, H5A and C15A, C19A) at 13.0 and 87.0 % occupancy, respectively.

Hydrogen atoms H1N, H2N, H3N, H4N H5N and H6N were found from a Fourier difference map and N–H distances were set at 0.87 (0.02) Å and allowed to refine with U_{iso} at 1.20 of parent N atom. All other hydrogen atoms were placed in calculated positions with C–H distances for CH of 1.00 Å, C(Ar)H 0.95 Å, and CH_3 of 0.98 Å with U_{iso} of 1.20 or 1.50 that of the parent C atom.

SHELXTL [18] and *Mercury* [19] programs were used to make the stereo drawings. Crystallographic data and details of structure refinement are listed in Table 1.

Tbale 1. Crystal data and structure refinement.

Empirical formula	$C_{13}H_{21}FN_3O_2P$
Formula weight	301.30
Temperature (K)	90 (2)
Wavelength (Å)	1.54178
Crystal system	Triclinic
Space group	$P\bar{1}$
Unit cell dimensions	a = 4.9312 (4) Å b = 17.7765 (16) Å c = 18.9829 (16) Å α = 108.651 (11)° β = 97.389 (7)° γ = 97.929 (7)°
Volume (Å^3)	1534.9 (2)
Z	4
Calculated density (g/cm^3)	1.304
Absorption coefficient (mm^{-1})	1.743
F(000)	640
Crystal size (mm^3)	0.35 × 0.08 × 0.08
Crystal color / habit	colourless / rod
Theta range for data collection (°)	2.67 to 61.34
Index ranges	$-5 \le h \le 4$ $-18 \le k \le 19$ $-20 \le l \le 19$
Reflections collected	6933
Independent reflections	4067 [R_{int} = 0.0458]
Completeness to theta = 25.00°	85.5%
Absorption correction	multi-scan / sadabs
Max. and min. transmission	0.8732 and 0.5806
Refinement method	Full-matrix least-squares on F^2
Data / restraints / parameters	4067 / 27 / 399
Goodness-of-fit on F^2	1.044
Final R indices [$I > 2\sigma(I)$]	R_1 = 0.0726, wR_2 = 0.1906
R indices (all data)	R_1 = 0.0961, wR_2 = 0.2049
Largest diff. peak and hole (e.Å^{-3})	0.777 and –0.674

2.2. Synthesis

The starting material 2-F-$C_6H_4C(O)NHP(O)Cl_2$ was prepared according to the literature method reported by Pourayoubi *et al.* [10].

For the preparation of studied compound, a solution of 2-F-$C_6H_4C(O)NHP(O)Cl_2$ (2 mmol) in CH_3CN (20 ml)

was added at 273 K to a solution of isopropylamine (8 mmol) in the same solvent (5 ml). After stirring for 4 h, the solvent was evaporated and the product was washed with distilled water. Colorless single crystals, suitable for X-ray diffraction experiment, were obtained at room temperature from a mixture of CH_3OH/CH_3CN (1:1 *v*/*v*).

3. Results and discussion

3.1. X-ray crystallography investigation

Selected geometrical parameters and details of the hydrogen bonding interactions for studied structure are summarized in Tables 2 and 3, respectively.

The asymmetric unit of studied structure consists of two complete molecules P1 and P2 (Fig. 1). Some of the carbon atoms in the isopropyl fragments and also, fluorine atoms of the 2-F-$C_6H_4C(O)$ fragments are disordered over two sets of sites.

Table 2. Selected geometric parameters (Å, º).

P1–O2	1.485 (4)	P2–O4	1.480 (4)
P1–N1	1.705 (5)	P2–N4	1.698 (5)
P1–N2	1.618 (5)	P2–N5	1.607 (5)
P1–N3	1.605 (5)	P2–N6	1.611 (5)
N1–C7	1.354 (7)	N4–C22	1.352 (7)
N2–C11	1.469 (8)	N5–C23	1.475 (8)
N3–C8	1.468 (8)	N6–C26	1.472 (7)
C7–O1	1.231 (6)	C22–O3	1.225 (6)
O2–P1–N1	103.3 (2)	O4–P2–N4	103.4 (2)
O2–P1–N2	115.1 (2)	O4–P2–N5	115.1 (3)
O2–P1–N3	116.5 (3)	O4–P2–N6	116.2 (2)
N1–P1–N2	111.0 (3)	N4–P2–N5	111.6 (2)
N1–P1–N3	107.7 (2)	N4–P2–N6	107.8 (3)
N2–P1–N3	103.2 (3)	N5–P2–N6	102.8 (3)
C7–N1–P1	124.8 (4)	C22–N4–P2	124.9 (4)
C11–N2–P1	125.1 (4)	C23–N5–P2	124.6 (4)
C8–N3–P1	123.4 (4)	C26–N6–P2	122.9 (4)
O1–C7–N1	121.5 (5)	O3–C22–N4	122.3 (5)
O2-P1-N1-C7	175.7 (4)	O4-P2-N4-C22	−176.7 (4)
N1-P1-N2-C11	69.9 (5)	N4-P2-N5-C23	−68.7 (5)
N1-P1-N3-C8	−62.9 (5)	N4-P2-N6-C26	62.4 (5)
P1-N1-C7-O1	−3.9 (8)	P2-N4-C22-O3	5.1 (8)

The P atoms display a distorted tetrahedral environment with the bond angles in the range of 103.2 (3)° – 116.5 (3)° for molecule P1 and 102.8 (3)° – 116.2 (2)° for molecule P2.

The P═O bond lengths and O═P–N and P–N–C bond angles are in the standard ranges of similar compounds [5,20]. The P–N_{CP} bond is longer than the two other P–N bonds [N_{CP} is introduced as the nitrogen atom of the C(O)NHP(O) part] and the C–N_{CP} bond is shorter than the two other C–N bonds, for example in molecule P1: P–N_{CP} = 1.705 (5) Å, P–N = 1.618 (5) Å and 1.605 (5) Å, and C–N_{CP} = 1.354 (7) Å, C–N = 1.469 (8) Å and 1.468 (8) Å. Moreover, the O–P–N_{CP} angles are smaller than the two related O–P–N angles, for example in molecule P2: ∠O4–P2–N4 = 103.4 (2)°, ∠O4–P2–N5 = 115.1 (3)° and ∠O4–P2–N6 = 116.2 (2)°.

Table 3. Hydrogen-bond geometry (Å, º).

D–H…*A*	*d*(*D*–H)	*d*(H…*A*)	*d*(*D*…*A*)	∠(*DHA*)
N2–H2N...O2^{i}	0.87 (7)	2.08 (7)	2.932 (6)	168 (6)
N5–H5N...O4^{ii}	0.76 (6)	2.24 (6)	2.935 (6)	153 (6)
N6–H6N...O4^{ii}	0.80 (7)	2.19 (7)	2.953 (6)	160 (7)
N3–H3N...O2^{i}	0.75 (6)	2.25 (6)	2.955 (7)	157 (6)
N1–H1N...O1^{ii}	0.75 (6)	2.17 (7)	2.902 (7)	164 (6)
N4–H4N...O3^{i}	0.69 (5)	2.23 (6)	2.906 (6)	166 (6)

Symmetry transformations used to generate equivalent atoms: (i): *x* + 1, *y*, *z*; (ii): *x* – 1, *y*, *z*.

In the structure of studied compound, the C═O and P═O groups (which are separated through the N_{CP} atom) adopt an *anti*-orientation relative to one another in both molecules P1 and P2. This situation leads to the *syn*-orientations of N_{CP}–H units with respect to the P═O groups; so, in the crystal, the N_{CP}–H···O═C and $(N–H)_2$···O═P hydrogen bonds lead to the formation of two independent one-dimensional aggregates (each including one independent molecule) along the *a* axis (Fig. 2) with forming the graph set $R_2^2(10)/R_2^1(6)$ [20] (for graph set notation, see ref. [21]).

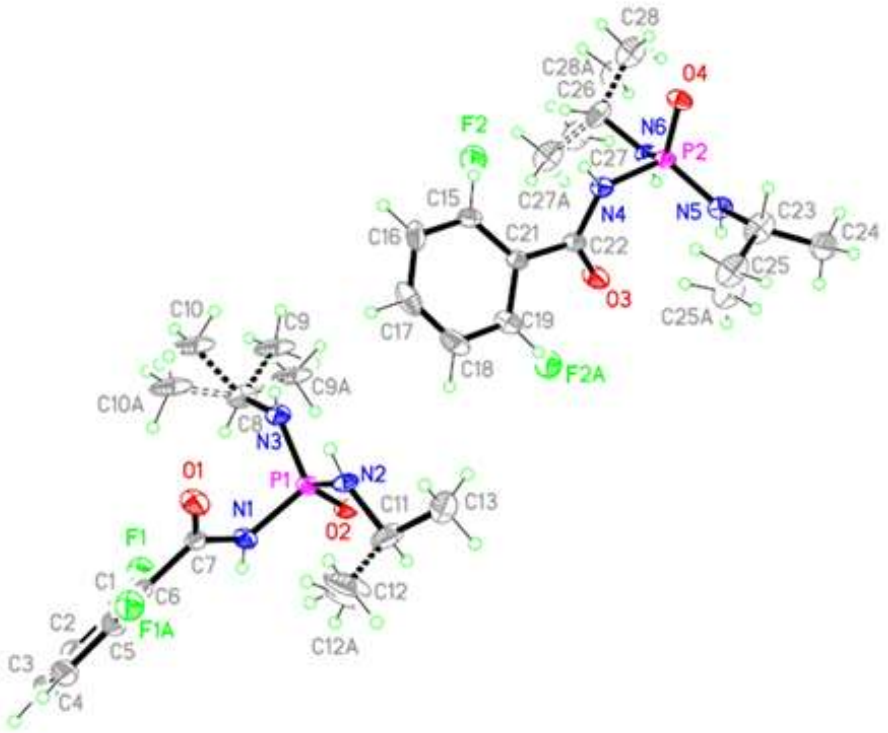

Fig. 1. The asymmetric unit of studied compound, showing the atom-labelling scheme for two molecules P1 and P2. Displacement ellipsoids are drawn at the 50% probability level and H atoms are drawn as circles of arbitrary radii. The minor disordered atoms with lower occupancy are labeled with the suffix 'A'.

In addition to the hydrogen bonds discussed, the structure may be rationalized by the weak cohesion from the C–H···O═P hydrogen bonds [C17–H17···O2═P1: C17···O2 = 3.422 (6) Å; symmetry code: x – 1, y, z and C3–H3A···O4═P2: C3···O4 = 3.431 (6) Å; symmetry code: x + 2, y + 1, z + 1]. These interactions lead to the formation of a 2D layer composed of two independent H-bonded chains (Fig. 3).

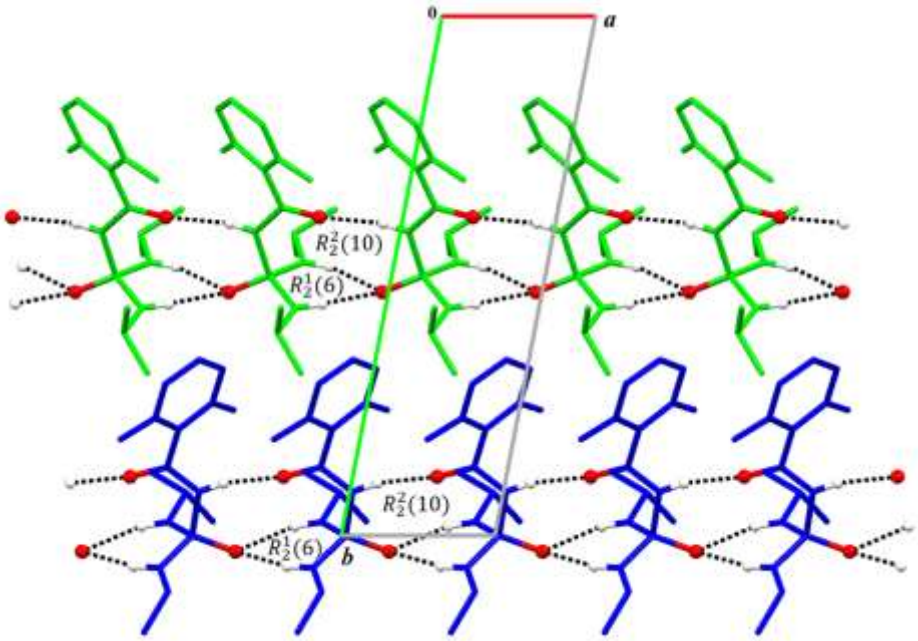

Fig. 2. A crystal packing diagram for studied structure is shown. 1D chains, along [100], are formed by the connection of adjacent independent molecules, *via* N_{CP}–H···O═C and [N–H]$_2$···O═P hydrogen bonds (black dashed lines) building $R_2^2(10)/R_2^1(6)$ ring motifs. Different colors are shown for different molecules P1 and P2. The contact atoms O and H are displayed as "balls" style and H atoms not involved in hydrogen bonding have been omitted for clarity.

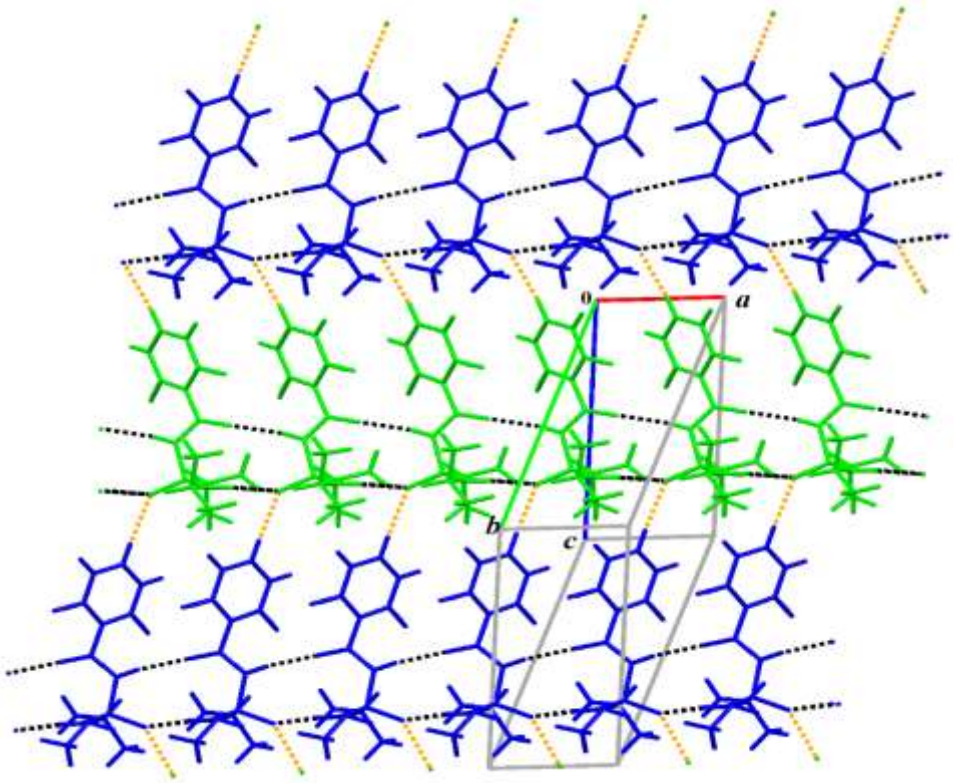

Fig. 3. Part of the crystal packing of studied structure is shown. A 2D layer is formed by connection of the independent chains (colored blue and green) through C–H···O=P hydrogen bonds (shown as orange dashed lines) parallel to the (04–4) plane.

3.2. Study of intermolecular interactions by Hirshfeld surface analysis

The analysis of molecular crystal structures using a visual tool based on Hirshfeld surfaces provides a new way of visualizing interactions in molecular crystals which offers a 3D picture of molecular shape in a crystalline environment [22]. When a Hirshfeld surface is proposed as an effective way to discern intermolecular interactions in the solid state, the first properties to be mapped on this surface are d_e and d_i which describe the distances from a point on the surface to the nearest nucleus outside and inside the surface, respectively [23]. A red-blue-white color scheme by the d_{norm} (normalized contact distances based on van der Waals radii) Hirshfeld surfaces is employed for comparison of intermolecular interactions in crystal structures: red regions represent contacts shorter than sum of van der Waals radii with negative d_{norm} values; white regions represent intermolecular distances close to van der Waals contacts with d_{norm} equal zero; and blue regions represent contacts longer than sum of van der Waals radii with positive d_{norm} values [24].

The Hirshfeld molecular surfaces of molecules P1 and P2 of studied compound were generated using *CrystalExplorer* 3.1 [13] basing on results of X-ray studies in CIF format. Bond lengths to hydrogen atoms were set to standard neutron values (C–H = 1.083 Å and N–H = 1.009 Å) during calculations. The normalized contact distances d_{norm} were mapped into the Hirshfeld surfaces (HSs), from –0.540 Å to +1.487 Å for P1 and from –0.540 Å to +1.468 Å for P2.

The most prominent features on HSs of molecules P1 and P2 are the deep red spots due to N–H···O hydrogen bonds (Table 3, Fig. 4), i.e. N–H_{CP}···O=C and N–H···O=P which are one of the most important features of the hydrogen bond patterns in the phosphoric triamides having a P(O)NHC(O) skeleton. There are also light red spots on the HSs which reflect the C–H···O and H…H interactions (Fig. 4). The weak C–H···O hydrogen bond is related to the interaction

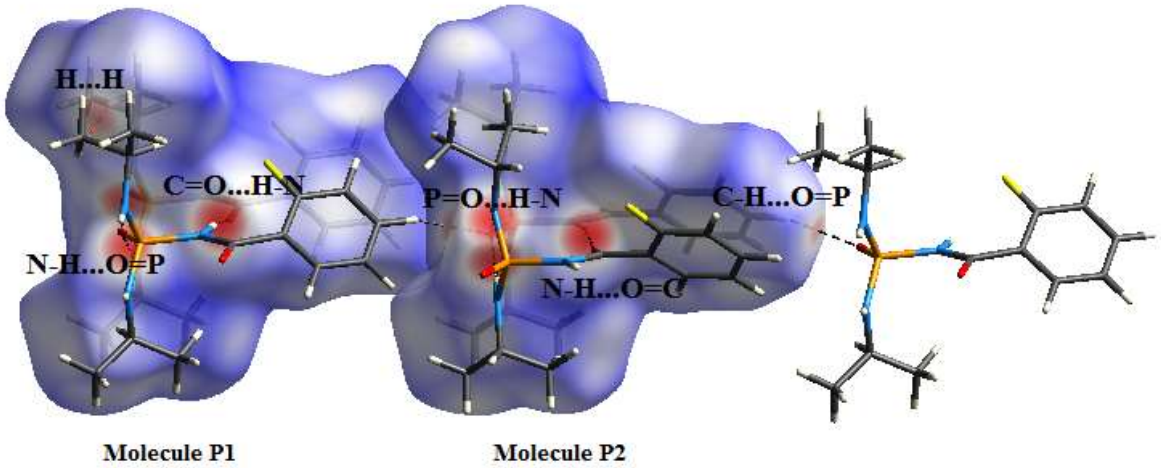

Fig. 4. A View of d_{norm} Hirshfeld surfaces plotted on the molecules P1 and P2 of the studied structure, surrounded by neighboring molecules associated with close contacts. The red spots are introduced by N–H···O, C–H···O and H···H interactions.

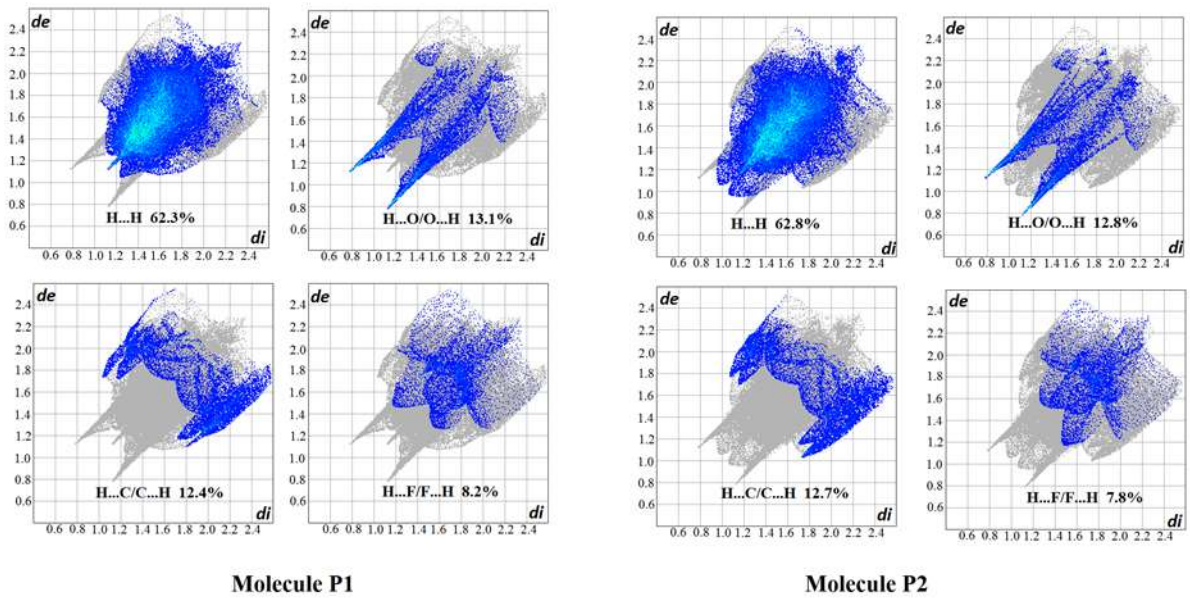

Fig. 5. Decomposed fingerprint plots and percentage contributions of various intermolecular H···H and H···X/X···H (X = O, C and F) contacts to the Hirshfeld surfaces of molecules P1 and P2. The full fingerprint plot appears as a grey shadow below each decomposed plot.

between the CH group of 2-F-C_6H_4 segment and the O atom of phosphoryl group, and the H···H contact refers to the weak Van der Waals interaction between the H atoms of CH_3 groups of isopropyl segments.

Fig. 5 shows the decomposed 2D fingerprint plots (FPs) of the HSs and the related percentage contributions of the intermolecular contacts for molecules P1 and P2. These plots were generated using a pair distance (d_e, d_i) for each individual surface spot and quantitatively summarize the information provided by the generated HSs in two dimensional histograms. The decomposed FPs include the reciprocal H···X/X···H contacts in which X atom is located outside (for H···X, $d_e > d_i$) or inside (for X···H, $d_e < d_i$) of the generated HS as an H-atom acceptor [25, 26].

For both molecules P1 and P2, the highest proportions of contacts, marked by the points spread out in a large area of FPs, are observed for H···H contacts (comprising 62.3% in P1 and 62.8% in P2). Moreover, the frequency of occurrence of H···H contacts in both molecules is

increased in the regions of $d_e \approx 1.1 – 1.9$ Å and $d_i \approx 1.1 – 1.7$ Å on the plot diagonal, shown as the bright areas colored from blue to green-blue. For molecule P1, a short spike is visible for the shortest H···H contacts (in $d_e = d_i \approx 1.1 – 1.2$ Å), whereas, such spike is not observed for molecule P2.

The H···O/O···H contacts containing the N–H···O hydrogen bonds show a pair of sharp spikes in the related decomposed FPs. These H···O/O···H contacts include 13.1% of the total HS area for P1 and 12.8% for P2, providing the closest contacts with minimum $d_i + d_e$ values of ≈ 1.9 for P1 and P2.

The H···C and C···H contacts combined cover the regions of top left ($d_e > d_i$, H···C) and bottom right ($d_e < d_i$, C···H) of the related plots in Fig. 5, comprising 12.4% of the surface for P1 and 12.7% for P2. The shape of these contacts can be described as two wing.

The H···F/F···H contacts include 8.2% (for molecule P1) and 7.8% (for molecule P2) of the surface. Other interactions such as F···O, C···O and C···C altogether comprise 4.0% and 3.9% of total HS areas for molecules P1 and P2, respectively. The related decomposed fingerprint plots of these contacts with minor contribution (≤ 1.0% for each contact) has not been shown in Fig. 5.

Finally, a visual inspection of FPs in Fig. 5 shows that the downer d_e and d_i values on the full FP of molecule P1 which cover the short H···H contacts are more compact than those in the full FP of molecule P2 (d_e, d_i (around the diagonal plot) < 1.1 Å in P1 and d_e, d_i < 1.0 Å in P2), indicating more important role of such interactions with low d_e and d_i distances in the crystal packing of P1 relative to P2. Moreover, by comparing the FPs in Fig. 5, it is seen that although the nature of intermolecular interactions in two independent molecules P1 and P2 are similar to each other, there are minor differences in the distribution of H···H, H···O/O···H, H···C/C···H and H···F/F···H interactions.

4. Conclusion

New phosphoric triamide [2-F-$C_6H_4C(O)NH]P(O)[NHCH(CH_3)_2]_2$ was synthesized and structurally characterized. 3D Hirshfeld surfaces and corresponding 2D fingerprint plots were employed to obtain the visual identification of various interactions within the structure. This study elucidated that the studied structure are stabilized mainly by H···H H···O/O···H, H···C/C···H and H···F/F···H contacts.

Acknowledgments

We thank Semnan University for supporting this study.

Supplementary Information

Crystallographic data (CIF) for the structure reported in this article has been deposited in the Cambridge Crystallographic Data Centre with the CCDC number of 973793. Copy of the data can be obtained, free of charge *via* www.ccdc.cam.ac.uk/data_request/cif.

References

[1] M.J. Domínguez, C. Sanmartín, M. Font, J.A. Palop, S. San Francisco, O. Urrutia, F. Houdusse, J.M. García-Mina, *J. Agric. Food Chem.* **56** (2008) 3721–3731.

[2] Z. Li, J. Han, Y. Jiang, P. Browne, R.J. Knox, L. Hu, *Bioorg. Med. Chem.* **11** (2003) 4171–4178.

[3] M. Pourayoubi, S. Shoghpour Bayraq, A. Tarahhomi, M. Nečas, K. Fejfarová, M. Dušek, *J. Organomet. Chem.* **751** (2014) 508–518.

[4] M. Pourayoubi, J.A. Golen, M. Rostami Chaijan, V. Divjakovic, M. Negari, A.L. Rheingold, *Acta Crystallogr*. C**67** (2011) m160–m164.

[5] A. Tarahhomi, M. Pourayoubi, A.L. Rheingold, J.A. Golen, *Struct. Chem.* **22** (2011) 201–210.

[6] A. Tarahhomi, M. Pourayoubi, J.A. Golen, P. Zargaran, B. Elahi, A.L. Rheingold, M.A. Leyva Ramírez, T. Mancilla Percino, *Acta Crystallogr.* B**69** (2013) 260–270.

[7] M. Keikha, M. Pourayoubi, A. Tarahhomi, A. van der Lee, *Acta Crystallogr*. C**72** (2016) 251–259.

[8] M.A. Spackman, D. Jayatilaka, *CrystEngCommun.* **11** (2009) 19–32.

[9] M.A. Spackman, J.J. McKinnon, *CrystEngCommun*. **4** (2002) 378–392.

[10] M. Pourayoubi, A. Tarahhomi, A.L. Rheingold, J.A. Golen, *Acta Crystallogr.* E**67** (2011) o934.

[11] A. Tarahhomi, M. Pourayoubi, A.L. Rheingold, J.A. Golen, *Acta Crystallogr.* E**67** (2011) o2643.

[12] M. Pourayoubi, A. Tarahhomi, A.L. Rheingold, J.A. Golen, *Acta Crystallogr.* C**70** (2014) 998–1002.

[13] S.K. Wolff, D.J. Grimwood, J.J. McKinnon, M.J. Turner, D. Jayatilaka, M.A. Spackman, *CrystalExplorer* 3.1, University of Western Australia, Crawley, Australia (2013).

[14] Bruker, *SMART* and *SAINT*. Bruker AXS Inc., Madison, Wisconsin, USA (2005).

[15] G.M. Sheldrick, *SADABS*. University of Göttingen, Germany (2004).

[16] Bruker, *APEXII* and *SADABS*. Bruker AXS Inc., Madison, Wisconsin, USA (2014).

[17] G.M. Sheldrick, *Acta Crystallogr.* A**64** (2008) 112–122.

[18] G.M. Sheldrick, *Acta Crystallogr.* C**71** (2015) 3–8.

[19] C.F. Macrae, I.J. Bruno, J.A. Chisholm, P.R. Edgington, P. McCabe, E. Pidcock, L. Rodriguez-Monge, R. Taylor, J. van de Streek, P.A. Wood, *J. Appl. Crystallogr*. **41** (2008) 466–470.

[20] M. Pourayoubi, A. Tarahhomi, A. Saneei, A.L. Rheingold, J.A. Golen, *Acta Crystallogr*. C**67** (2011) o265–o272.

[21] M.C. Etter, J.C. MacDonald, J. Bernstein, *Acta Crystallogr*. B**46** (1990) 256–262.

[22] J.J. McKinnon, F.P.A. Fabbiani, M.A. Spackman, *Cryst. Growth. Des.* **7** (2007) 755–769.

[23] A.D. Martin, J. Britton, T.L. Easun, A.J. Blake, W. Lewis, M. Schröder, *Cryst. Growth. Des.* **15** (2015) 1697–1706.

[24] J.J. McKinnon, A.S. Mitchell, M.A. Spackman, *Chem. Eur. J.* **4** (1998) 2136–214.

[25] J.J. McKinnon, M.A. Spackman, A.S. Mitchell, *Acta Crystallogr*. B**60** (2004) 627–668.

[26] F.P.A. Fabbiani, C.K. Leech, K. Shankland, A. Johnston, P. Fernandes, A.J. Florence, N. Shankland, *Acta Crystallogr*. C**63** (2007) o659–o663.